

Whisker Formation on Electroplated Sn-Cu

*M. E. Williams, C. E. Johnson, K.-W. Moon, G. R. Stafford, C. A. Handwerker,
and W. J. Boettinger
Metallurgy Division, MSEL/ NIST/ Gaithersburg/ MD 20899-8555/ USA*

The probability of whisker growth on as-deposited tin (Sn) electrodeposits has been measured as a function of copper (Cu^{2+}) addition to a commercial bright methanesulfonate electrolyte. Two substrate materials were used: free standing 250 μm thick pyrophosphate Cu and 40 nm thick fine grain Cu evaporated on silicon (Si)(100) wafer. Deposits 3 μm thick and 3 cm^2 in area with average composition between 0 % and 1.6 % mass fraction Cu were produced from Cu^{2+} electrolyte concentrations between 0 and 25×10^{-3} mol/L respectively at 60 mA/cm^2 in a rotating disk geometry.

Whisker defects were not observed on any of the pure Sn deposits regardless of substrate, nor were they present on Sn-Cu films deposited on the evaporated Cu on Si(100) substrate. However, whiskers started to grow after only 2 days on the Sn-Cu films deposited on the pyrophosphate Cu substrates. Detailed measurements over 12% of the deposit areas after one year of room temperature storage show a defect density of less than 5 $/\text{mm}^2$ for compositions below 0.25 % mass fraction Cu, but a density of approximately 40 $/\text{mm}^2$ for compositions above 0.7 % mass fraction Cu. The effect of Cu content and substrate material on the defect density is discussed.

For further information contact:
M. E. Williams
Metallurgy Division
NIST
Gaithersburg, MD 20899 USA
1-301-975-6170
maureen.williams@nist.gov

1. Introduction

Tin(Sn)-lead(Pb) alloys have been used extensively for surface finishing of electronic components in part because Pb was found to be effective in retarding Sn whisker growth in electrodeposits. Since lead-free solder alloys have been introduced, electronic manufacturers are seeking a new surface finish technology that will prevent Sn whisker growth without the use of Pb.

There have been several studies to understand the Sn whisker growth mechanism that focus on residual stress generation by intermetallic compound formation with the underlying substrate^[1-3]. Some of the other key factors that have been found to influence Sn whisker growth are: deposit thickness,^[4] deposit stress levels,^[5] substrate stress levels,^[6] additives,^[7] grain size and shape,^[8] and interdiffusion barriers^[9]. In spite of this wealth of information, basic understanding of whisker growth and its prevention remains primitive. We have focused on the influence of Cu²⁺ concentration in the electrolyte on whisker defect density.

2. Experimental Procedure

2-1. Electrodeposition

Two different types of Cu substrate were prepared for Sn electroplating in order to examine their effects on deposit microstructure and Sn whisker growth. One was a free standing sample of electrodeposited copper, 250 μm thick, made from a pyrophosphate electrolyte. The second was a 40 nm thick evaporated Cu film on a Si(100) wafer. The pyrophosphate copper substrates were prepared by polishing, degreasing, magnesium oxide scrubbing, deionized water rinsing and air blast drying. The evaporated Cu substrates were not polished. Prior to tin electroplating, all substrates were immersed in 25 % sulfuric acid solution for 5 seconds to remove the oxide film and rinsed by deionized water.

Bright coatings of Sn and Sn-Cu alloys were electrodeposited from a commercial methanesulfonate electrolyte. The electrolyte was prepared with high purity water with a resistivity of 18.3 M Ω -cm. A rotating disk electrode assembly was employed at 100 rpm to provide reproducible plating conditions and to approximate flow conditions in commercial strip plating. The 3 cm² samples were plated at a constant current density of 60 mA/cm² in one liter of solution at 25 °C \pm 0.5 °C to a thickness of 3 μm . This correlates to a growth rate of approximately 0.05 μm / sec. The anode was a 99.999 % Sn sheet. The Cu²⁺ concentration in the electrolyte was varied from 0 to 25 x 10⁻³ mol/L by the addition of copper methanesulfonate [Cu(CH₃SO₃)₂].

2-2. Analysis

The deposit surface grain size was measured by the grid-intercept method from a 13 μm x 10 μm region near the center of the deposit using a 3 line x 4 line grid^[10]. To determine the Cu composition in the deposits, energy dispersive x-ray spectroscopy (EDS) analysis was performed on cross sections of 10 μm thick Sn films that had been electrodeposited onto Cu evaporated Si(100). Thicker deposits were required for EDS to facilitate the analysis. The cross sections

were carefully polished in separate mounts to eliminate Cu contamination. Because the deposits were multiphase, EDS data were acquired from twenty $3\ \mu\text{m} \times 16\ \mu\text{m}$ areas to obtain an average over the two phases. The Cu contents of selected deposits were also measured by Inductively Coupled Plasma Spectrometry (ICP). Free standing films were obtained by electrodepositing Sn and Sn-Cu on amorphous carbon substrates under identical conditions as those deposited for the whisker study. Each deposit was completely dissolved in concentrated HNO_3 and the average compositional value was obtained from the results of ten scans.

In this study, surface defects are defined as including whiskers (Figure 1(a)) and eruptions (Figure 1(b)). Defect densities were measured on $3\ \mu\text{m}$ thick electrodeposits. Preliminary measurement of the defect density at short times (< 24 days) has been previously reported^[11]. These measurements covered only 0.1 % of the circular deposit area. In the present paper, 12% of total deposit area was inspected yielding much tighter statistics. Five strips centered along parallel chords of the circular electrodeposits were examined using optical microscopy.

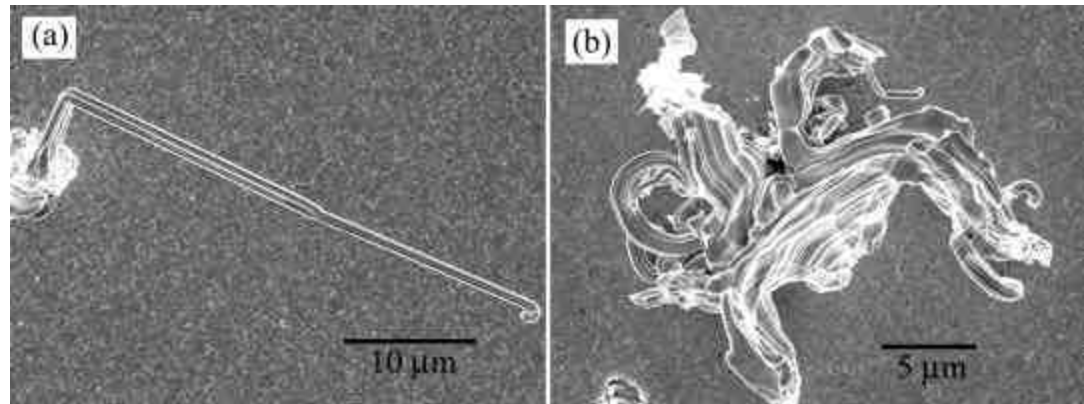


Figure 1: Types of defects on the Sn deposit; (a) a filament type Sn whisker and (b) a Sn eruption with small length whisker.

3. Results

3-1. Cu content of the deposits

The Cu contents of the films determined by both methods are given in Table 1. The ICP method, which is considered more reliable for these multiphase materials, gave Cu contents approximately one half of those obtained by EDS. The Cu content of samples not directly analyzed by the ICP method (* in table) were estimated through a linear fit of EDS to ICP data.

Table 1. Summary of Measurements

Cu ²⁺ in electrolyte (mol/L)	Cu in deposit (mass %) EDS	Cu in deposit (mass %) ICP	Sn surface grain size (μm)	Defect Density after 1 year (mm ⁻²)	Longest Whisker Observed (μm)
0	0	0.04 ± 0.01	0.64±0.05	0	-
0.00050	0.29±0.33	0.05 ± 0.02	0.60±0.05	1.6 ± 0.9	15
0.00275	0.67±0.38	0.25 ± 0.2*	0.57±0.06	5.1 ± 1.8	37
0.00500	1.49±0.42	0.67 ± 0.2*	0.58±0.10	48 ± 9	400
0.00750	1.42±0.45	0.67 ± 0.04	0.55±0.09	32 ± 11	400
0.01500	2.93±1.15	1.42 ± 0.06	0.31±0.03	42 ± 12	1600
0.02500	3.28±0.92	1.61 ± 0.49*	0.19±0.02	32 ± 11	1050

*Not analyzed; values estimated from linear fit of EDS to ICP values of other samples.

Figure 2 shows that the Cu content in the Sn deposit increases as a function of the Cu²⁺ concentration in the electrolyte. From Figure 2, it is clear that the Cu is not depositing at the mass-transport-limited current; otherwise, Figure 2 would show a linear dependence of alloy composition on the Cu²⁺ concentration [12]. We have observed an immersion deposit of Cu on the Sn anodes when the Cu²⁺ concentration in the electrolyte exceeds 25 x 10⁻³ mol/L, and have attributed this to an insufficient amount of Cu²⁺ complexing agent in the electrolyte. The limit on the electroactive Cu²⁺ concentration in the electrolyte limits the Cu content in the deposit.

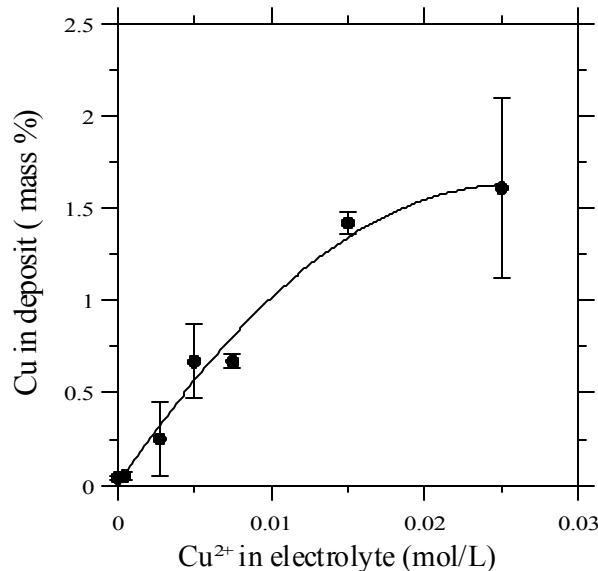


Figure 2. Cu content in the Sn deposit (as determined by ICP) as a function of Cu²⁺ concentration in the electrolyte. The deposits were formed at a constant current density of 60 mA/cm² on a rotating disk electrode at 100 rpm.

The equilibrium solubility of Cu in body centered tetragonal (bct) Sn is very small. Its measured value at 227°C is only 0.0063 % mass fraction Cu^[13] and is estimated as 10 times smaller at room temperature^[14]. Electrodeposition usually produces metastable supersaturated solid solutions. The

supersaturation is relieved soon after deposition by the formation of Cu_6Sn_5 particles that would be expected to form on the Sn grain boundaries. The increase in the standard deviation of the EDS measured Cu contents in Table 1 at the higher Cu compositions is most likely a reflection of the inhomogeneity of the electrodeposits as they become a two-phase mixture.

3-2. Defect density

In this study, we have observed two types of defects on the electrodeposited Sn film: Sn whiskers (Figure 1(a)) and eruptions (Figure 1(b)). Whiskers grow out of earlier forming eruptions, but not all eruptions lead to whiskers. From the observation based on substrate types and aging time of one year, defects were not observed on any of the pure Sn deposits regardless of substrate, nor were they present on Sn-Cu films deposited on the Cu evaporated on Si(100) substrate. However, whiskers started to grow after 2 days from the Sn-Cu deposits on the pyrophosphate Cu substrate. A summary of the whisker density and longest whiskers is also given in Table 1.

3-3. Deposit microstructure

In a previous paper, Moon et al.^[11], it was shown that the pyrophosphate Cu substrate led to a preferred Sn orientation of (103) while the Cu evaporated Si(100) substrate led to a preferred Sn orientation of (101). Alloying the Sn with up to 1.6 % mass fraction of Cu did not influence the preferred orientation of the Sn deposits.

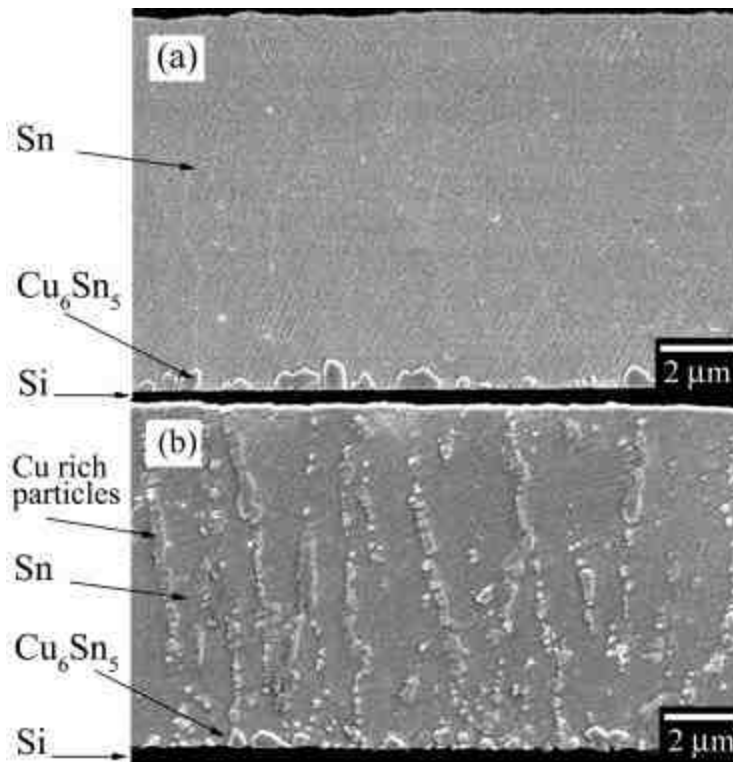


Figure 3. SEM cross section micrographs of unetched 10 μm thick deposits on Cu coated Si a) pure Sn; b) Sn 0.67 % mass fraction Cu.

Figure 3 shows cross sections of two electrodeposits: pure Sn and Sn-0.67 % mass fraction Cu. Intermetallic Cu_6Sn_5 forms on the Cu coated Si in both samples (seen at the bottom of the micrographs). In addition, Cu-rich particles, also identified as Cu_6Sn_5 , are seen in the bulk of the alloy deposit. The Cu_6Sn_5 particles decorate the boundaries of the Sn grains that are predominantly columnar.

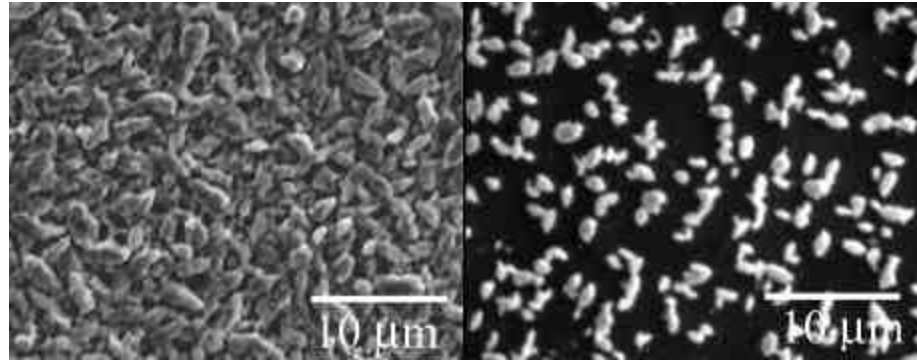


Figure 4. SEM micrographs of Cu_6Sn_5 intermetallic remaining after removal of pure Sn electrodeposit on: a) pyrophosphate Cu substrate and b) Cu on Si substrate. The black area in b) is Si indicating that the 40 nm layer has been completely consumed by the intermetallic formation.

Note in Figure 3 that the intermetallic does not completely cover the substrate for the deposits on the Cu coated Si. To examine this in more detail, the electrodeposit was removed by etching in concentrated HCl. SEM micrographs (Figure 4) show that the intermetallic particles completely cover the pyrophosphate Cu substrate but many areas of Si are exposed on the Cu coated Si substrate. Apparently the Cu was completely consumed by intermetallic formation in the latter, and there was insufficient Cu to completely cover the surface with intermetallic.

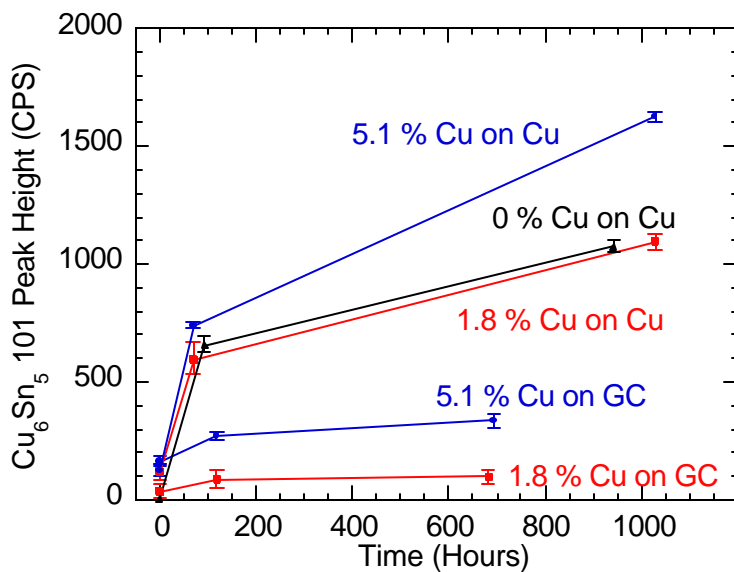


Figure 5. Intensity of Cu_6Sn_5 101 peak as a function of time from $1\ \mu\text{m}$ thick pure Sn and Sn-Cu electrodeposits on glassy carbon and Cu substrates.

An additional set of experiments confirms that Cu_6Sn_5 intermetallic compound forms in the bulk of Sn-Cu alloy deposits. The rate of intermetallic formation was estimated from x-ray diffraction patterns of Sn-Cu electrodeposits measured over a period of 1000 hrs after deposition. Figure 5 is a plot of the peak intensity of the Cu_6Sn_5 101 reflection for $1\ \mu\text{m}$ thick alloys containing 1.8 % and 5.1 % mass fraction Cu, deposited on either copper or glassy carbon substrates. For both substrate materials, the x-ray data indicates that Cu_6Sn_5 is present in the alloy within 15 minutes after deposition. For alloys deposited onto glassy carbon, Cu_6Sn_5 is exclusively formed from supersaturated bct Sn and its precipitation is essentially complete after a few days. These are the particles that are seen to decorate the grain boundaries in Figure 3(a). When identical deposits are formed on copper substrates, the amount of Cu_6Sn_5 formed on the deposit-substrate interface far exceeds that formed in the bulk deposit. The interfacial Cu_6Sn_5 continues to form long after bulk intermetallic formation is complete, as long as there is sufficient Sn and Cu at the interface.

3-4 Surface morphology and grain size ($3\ \mu\text{m}$ thick Sn deposits)

Figure 6 shows SEM micrographs of the as-deposited surface as a function of the Cu content for $3\ \mu\text{m}$ thick films electrodeposited on the pyrophosphate Cu substrate. The surface grain size (reported in Table 1) is approximately $0.6\ \mu\text{m}$ for alloys containing up to 0.67 % mass fraction Cu. This is essentially unchanged from that of the pure Sn deposit. The data shows that there is a relatively large distribution of grain sizes in this composition range, as indicated by the large standard deviations. When the alloy composition exceeds 0.67 % mass fraction Cu, the surface grain size drops rather significantly and the grains appear to become more uniform (smaller standard deviation).

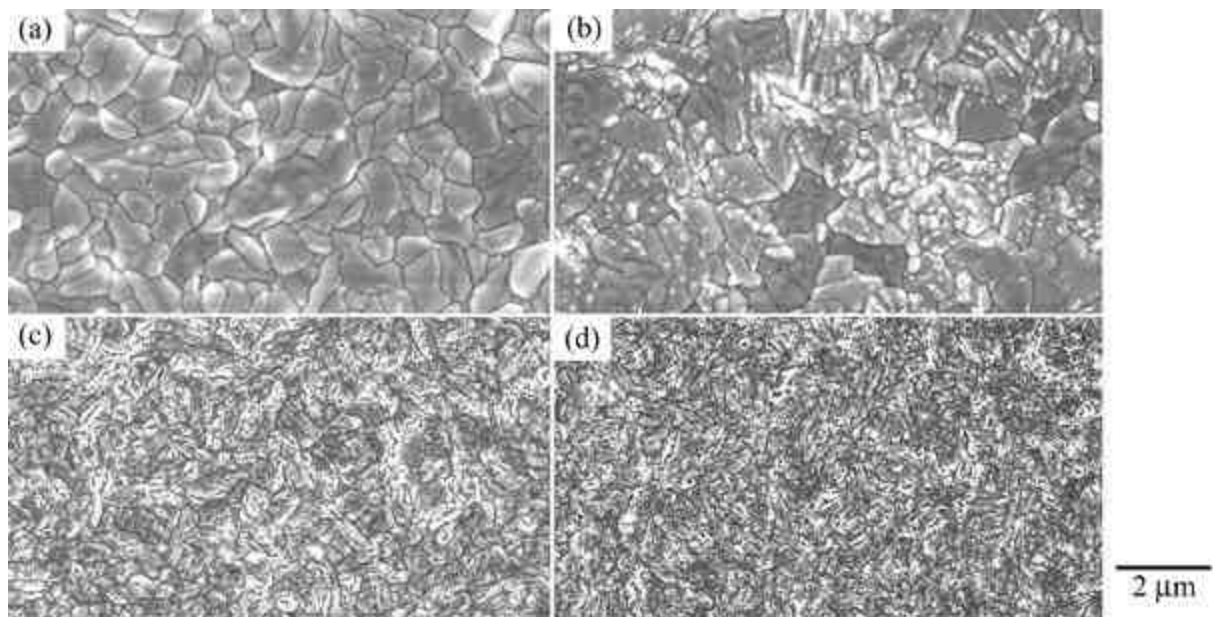


Figure 6. SEM micrographs of the as-deposited surface of 3 μm thick Sn-Cu electrodeposits containing a) 0 %, b) 0.67 %, c) 1.42 %, d) 1.6 % mass fraction Cu.

4. Discussion and Conclusion

The major observation of this paper is that no whiskers were observed in pure Sn electrodeposits. This appears to be in conflict with many commercial observations. The electrolyte used in the present experiments contains 0.8 ppm (mass) Cu (actual lot analysis from vendor). In commercial practice, electrolytes can contain up to 300 ppm (mass) Cu^{2+} (5×10^{-3} mol/L). According to Table 1, 5×10^{-3} mol/L Cu^{2+} would be in the range where whiskers can be expected.

We suggest several reasons why Cu additions enhance whisker formation. As described above the Cu in the electrodeposit is found as intermetallic Cu_6Sn_5 particles along grain boundaries. First, the formation of these precipitates from the supersaturated Sn solid solution can produce residual stress in the remaining Sn matrix. Second, the presence of the particles will greatly increase the flow stress of the deposit and let more residual stress be stored in the deposit. Third, the particles may retard the stress relaxation processes that would normally occur in pure Sn. Further research on this subject is required.

The second major observation is the dramatic difference between the two substrate materials. No whiskers form on the Cu coated Si substrate. Because the Cu was only 40 nm thick, the entire Cu layer is converted to intermetallic with regions of bare Si against electrodeposit. Thus debonding may occur leading to relaxation of the residual stresses in the film and the suppression of whisker formation. Preliminary experiments using thicker Cu seem to support this conclusion.

Reference

1. B.Z. Lee and D. N. Lee; *Acta Materialia*, 46 (10), (1998) pp. 3701-3714.
2. K.N. Tu; *Physical Review B-Condensed Matter*, 49 (3) (1994) pp. 2030-2034.

3. U. Lindborg; *Acta Metallurgica* , 24 (2): (1976) pp. 181-186.
4. S.M. Arnold; *Plating*, 1 (53) (1966) pp. 96-99.
5. K.N. Tu; *Acta Metallurgica*, 21 (1973) pp. 347-354.
6. N. Furuta, and K. Hamamura; *Japanese Journal of Applied Physics*, 8 (12) (1969) pp. 1404-1410.
7. D.W. Endicott and K.T. Kisner; "A Proposed Mechanism for Metallic Whisker Growth." *Proceedings of the 71st AES Annual Tech. Conf.*, (Amer. Electroplaters' Society, Inc.1984) pp. J-5-1-20.
8. T. Kakeshita, K. Shimizu, R. Kawanaka, and T. Hasegawa; *Journal of Materials Science*, 17 (9) (1982) pp.2560-2566.
9. R. Schetty; "Minimization of Tin whisker Formation for Lead-Free Electronic Finishing." *Proceedings of IPC Works 2000 (IPC, 2000)* pp. S-02-3-1 - 6.
10. H.E. Boyer and T.L. Gall: *Metals Handbook*, 9th Ed, (Metals Park: American Society for Metals, 1985) Section 35, p.18.
11. K-W. Moon, M.E. Williams, C.E. Johnson, G.R. Stafford, C.A. Handwerker, and W.J. Boettinger, *Proceedings of the Fourth Pacific Rim International Conference on Advanced Materials and Processing*, The Japanese Institute of Metals, Sendai, Japan, 2001, S. Hanada, Z. Zhong, S. W. Nam and R. N. Wright, eds., pp. 1115-1118.
12. A. J. Bard and L.R Faulkner; *Electrochemical Methods: Fundamentals and Applications*, (New York: John Wiley and Sons, Ltd., 1980) pp. 288.
13. C.E. Homer and H. Plummer, *J. Inst. Metals*, 64 (1939), pp.169-200.
14. U.R. Kattner, NIST , Gaithersburg, MD, 2002, unpublished research.

Appendix 1 – Results by Whisker Classification

Deposit	Substrate	Barrier Layer	Thickness, μm	Annealed	Whiskers Observed (Type 0, 1, 2, 3, or 4)				Index
					As-is	1 month	2 months	3 months	
Matte 90/10 tin/lead	Brass	None	3	N	0	0	0	0	0
Matte 90/10 tin/lead	Olin 194	None	3	N	0	0	0	0	0
Matte 90/10 tin/lead	Alloy 42	None	3	N	0	0	0	0	0
Matte 90/10 tin/lead	Brass	Copper, 5 μm	3	N	0	0	0	0	0
Matte 90/10 tin/lead	Brass	Nickel, 2 μm	3	N	0	0	0	0	0
Matte 90/10 tin/lead	Olin 194	Copper, 5 μm	3	N	2	2	2	2	5
Matte 90/10 tin/lead	Olin 194	None	10	N	0	0	0	0	0
Matte pure tin (1)	Brass	None	3	N	0	4	4	4	6
Matte pure tin (1)	Olin 194	None	3	N	4	4	4	4	10
Matte pure tin (1)	Alloy 42	None	3	N	1	1	4	4	4.75
Matte pure tin (1)	Brass	Copper, 5 μm	3	N	4	4	4	4	10
Matte pure tin (1)	Brass	Nickel, 2 μm	3	N	0	0	0	1	0.25
Matte pure tin (1)	Olin 194	Copper, 5 μm	3	N	4	4	4	4	10
Matte pure tin (1)	Olin 194	None	10	N	0	0	0	4	1
Matte pure tin (1)	Olin 194	None	10	Y	0	0	0	0	0
Matte pure tin (2)	Brass	None	3	N	0	4	4	4	6
Matte pure tin (2)	Olin 194	None	3	N	2	2	2	2	5
Matte pure tin (2)	Alloy 42	None	3	N	1	1	2	2	3.25
Matte pure tin (2)	Brass	Copper, 5 μm	3	N	4	4	4	4	10
Matte pure tin (2)	Brass	Nickel, 2 μm	3	N	1	1	1	1	2.5
Matte pure tin (2)	Olin 194	Copper, 5 μm	3	N	4	4	4	4	10
Matte pure tin (2)	Olin 194	None	10	N	1	1	1	1	2.5
Matte pure tin (2)	Olin 194	None	10	Y	0	0	0	2	0.5
Matte pure tin (3)	Brass	None	3	N	0	3	3	3	4.5
Matte pure tin (3)	Olin 194	None	3	N	2	2	2	2	5
Matte pure tin (3)	Alloy 42	None	3	N	0	0	2	4	2
Matte pure tin (3)	Brass	Copper, 5 μm	3	N	3	3	3	3	7.5
Matte pure tin (3)	Brass	Nickel, 2 μm	3	N	0	0	0	0	0
Matte pure tin (3)	Olin 194	Copper, 5 μm	3	N	3	3	3	3	7.5
Matte pure tin (3)	Olin 194	None	10	N	0	0	0	0	0
Matte pure tin (3)	Olin 194	None	10	Y	0	0	0	0	0
Matte tin/copper (1), 1% Cu	Brass	None	3	N	0	3	3	3	4.5
Matte tin/copper (1), 1% Cu	Olin 194	None	3	N	4	4	4	4	10
Matte tin/copper (1), 1% Cu	Alloy 42	None	3	N	0	1	1	1	1.5
Matte tin/copper (1), 1% Cu	Brass	Copper, 5 μm	3	N	4	4	4	4	10
Matte tin/copper (1), 1% Cu	Brass	Nickel, 2 μm	3	N	0	0	0	0	0
Matte tin/copper (1), 1% Cu	Olin 194	Copper, 5 μm	3	N	4	4	4	4	10
Matte tin/copper (1), 1% Cu	Olin 194	None	10	N	4	3	4	4	9.25
Matte tin/copper (1), 1% Cu	Olin 194	None	10	Y	0	0	0	0	0
Matte tin/copper (1), 4% Cu	Brass	None	3	N	2	4	4	4	8
Matte tin/copper (1), 4% Cu	Olin 194	None	3	N	4	4	4	4	10
Matte tin/copper (1), 4% Cu	Alloy 42	None	3	N	0	0	3	3	2.25
Matte tin/copper (1), 4% Cu	Brass	Copper, 5 μm	3	N	4	4	4	4	10
Matte tin/copper (1), 4% Cu	Brass	Nickel, 2 μm	3	N	0	0	0	0	0
Matte tin/copper (1), 4% Cu	Olin 194	Copper, 5 μm	3	N	4	4	4	4	10
Matte tin/copper (1), 4% Cu	Olin 194	None	10	N	4	4	4	4	10
Matte tin/copper (1), 4% Cu	Olin 194	None	10	Y	0	0	0	0	0
Matte tin/copper (2), 1% Cu	Brass	None	3	N	0	3	3	4	4.75
Matte tin/copper (2), 1% Cu	Olin 194	None	3	N	3	3	3	3	7.5
Matte tin/copper (2), 1% Cu	Alloy 42	None	3	N	0	0	4	4	3
Matte tin/copper (2), 1% Cu	Brass	Copper, 5 μm	3	N	4	4	4	4	10
Matte tin/copper (2), 1% Cu	Brass	Nickel, 2 μm	3	N	0	0	0	0	0
Matte tin/copper (2), 1% Cu	Olin 194	Copper, 5 μm	3	N	2	2	2	2	5
Matte tin/copper (2), 1% Cu	Olin 194	None	10	N	2	2	2	3	5.25
Matte tin/copper (2), 4% Cu	Brass	None	3	N	0	1	1	2	1.75
Matte tin/copper (2), 4% Cu	Olin 194	None	3	N	4	2	2	2	7
Matte tin/copper (2), 4% Cu	Alloy 42	None	3	N	0	2	4	4	4.5
Matte tin/copper (2), 4% Cu	Brass	Copper, 5 μm	3	N	1	1	1	1	2.5
Matte tin/copper (2), 4% Cu	Brass	Nickel, 2 μm	3	N	0	0	2	3	1.75
Matte tin/copper (2), 4% Cu	Olin 194	Copper, 5 μm	3	N	3	3	3	3	7.5
Matte tin/copper (2), 4% Cu	Olin 194	None	10	N	2	4	4	4	8

Appendix 1 - continued

Deposit	Substrate	Barrier Layer	Thickness, μm	Annealed	Whiskers Observed (Type 0, 1, 2, 3, or 4)				Index
					As-is	1 month	2 months	3 months	
Matte tin/bismuth, 2% Bi	Brass	None	3	N	0	2	2	2	3
Matte tin/bismuth, 2% Bi	Olin 194	None	3	N	0	1	2	2	2.25
Matte tin/bismuth, 2% Bi	Alloy 42	None	3	N	0	3	4	4	5.25
Matte tin/bismuth, 2% Bi	Brass	Copper, 5 μm	3	N	0	0	0	3	0.75
Matte tin/bismuth, 2% Bi	Brass	Nickel, 2 μm	3	N	0	0	0	0	0
Matte tin/bismuth, 2% Bi	Olin 194	Copper, 5 μm	3	N	0	0	0	2	0.5
Matte tin/bismuth, 2% Bi	Olin 194	None	10	N	0	0	0	2	0.5
Matte tin/bismuth, 5% Bi	Brass	None	3	N	0	0	1	1	0.75
Matte tin/bismuth, 5% Bi	Olin 194	None	3	N	0	0	0	2	0.5
Matte tin/bismuth, 5% Bi	Alloy 42	None	3	N	0	0	0	2	0.5
Matte tin/bismuth, 5% Bi	Brass	Copper, 5 μm	3	N	0	0	0	0	0
Matte tin/bismuth, 5% Bi	Brass	Nickel, 2 μm	3	N	0	0	0	2	0.5
Matte tin/bismuth, 5% Bi	Olin 194	Copper, 5 μm	3	N	0	0	0	3	0.75
Matte tin/bismuth, 5% Bi	Olin 194	None	10	N	0	0	0	0	0
Matte tin/bismuth, 10% Bi	Brass	None	3	N	0	0	0	0	0
Matte tin/bismuth, 10% Bi	Olin 194	None	3	N	0	0	0	0	0
Matte tin/bismuth, 10% Bi	Alloy 42	None	3	N	0	0	0	2	0.5
Matte tin/bismuth, 10% Bi	Brass	Copper, 5 μm	3	N	0	0	0	2	0.5
Matte tin/bismuth, 10% Bi	Brass	Nickel, 2 μm	3	N	0	0	0	0	0
Matte tin/bismuth, 10% Bi	Olin 194	Copper, 5 μm	3	N	0	0	1	2	1
Matte tin/bismuth, 10% Bi	Olin 194	None	10	N	0	0	0	0	0
Bright 90/10 tin/lead	Brass	None	3	N	0	0	0	0	0
Bright 90/10 tin/lead	Olin 194	None	3	N	0	0	0	0	0
Bright 90/10 tin/lead	Alloy 42	None	3	N	0	0	0	0	0
Bright 90/10 tin/lead	Brass	Copper, 5 μm	3	N	0	0	0	0	0
Bright 90/10 tin/lead	Brass	Nickel, 2 μm	3	N	0	0	0	0	0
Bright 90/10 tin/lead	Olin 194	Copper, 5 μm	3	N	0	0	0	0	0
Bright 90/10 tin/lead	Olin 194	None	10	N	0	0	0	0	0
Bright pure tin (1)	Brass	None	3	N	0	2	2	2	3
Bright pure tin (1)	Olin 194	None	3	N	2	4	3	2	7
Bright pure tin (1)	Alloy 42	None	3	N	0	0	0	0	0
Bright pure tin (1)	Brass	Copper, 5 μm	3	N	1	1	2	2	3.25
Bright pure tin (1)	Brass	Nickel, 2 μm	3	N	0	0	0	0	0
Bright pure tin (1)	Olin 194	Copper, 5 μm	3	N	4	4	4	4	10
Bright pure tin (1)	Olin 194	None	10	N	0	4	4	4	6
Bright pure tin (2)	Brass	None	3	N	0	0	2	2	1.5
Bright pure tin (2)	Olin 194	None	3	N	0	0	0	0	0
Bright pure tin (2)	Alloy 42	None	3	N	0	0	0	0	0
Bright pure tin (2)	Brass	Copper, 5 μm	3	N	2	2	2	2	5
Bright pure tin (2)	Brass	Nickel, 2 μm	3	N	0	0	0	0	0
Bright pure tin (2)	Olin 194	Copper, 5 μm	3	N	0	0	2	2	1.5
Bright pure tin (2)	Olin 194	None	10	N	0	0	1	1	0.75
Bright pure tin (3)	Brass	Nickel, 2 μm	3	N	0	0	0	0	0
Bright pure tin (3)	Olin 194	None	3	N	0	0	0	0	0
Bright pure tin (3)	Olin 194	None	10	N	0	0	0	0	0
Bright tin/copper (1), 2% Cu	Brass	None	3	N	0	2	2	2	3
Bright tin/copper (1), 2% Cu	Olin 194	None	3	N	0	0	0	0	0
Bright tin/copper (1), 2% Cu	Alloy 42	None	3	N	0	0	0	0	0
Bright tin/copper (1), 2% Cu	Brass	Copper, 5 μm	3	N	4	4	4	4	10
Bright tin/copper (1), 2% Cu	Brass	Nickel, 2 μm	3	N	0	0	0	0	0
Bright tin/copper (1), 2% Cu	Olin 194	Copper, 5 μm	3	N	2	2	2	2	5
Bright tin/copper (1), 2% Cu	Olin 194	None	10	N	0	0	0	0	0
Matte tin/silver, 2% Ag	Brass	None	3	N	0	4	4	4	6
Matte tin/silver, 2% Ag	Olin 194	None	3	N	0	0	0	2	0.5
Matte tin/silver, 2% Ag	Alloy 42	None	3	N	0	2	4	4	4.5
Matte tin/silver, 2% Ag	Brass	Copper, 5 μm	3	N	4	4	4	4	10
Matte tin/silver, 2% Ag	Brass	Nickel, 2 μm	3	N	2	2	2	3	5.25
Matte tin/silver, 2% Ag	Olin 194	Copper, 5 μm	3	N	3	4	4	4	9
Matte tin/silver, 2% Ag	Olin 194	None	10	N	0	0	0	0	0

Appendix 1 - continued

Deposit	Substrate	Barrier Layer	Thickness, μm	Annealed	Whiskers Observed (Type 0, 1, 2, 3, or 4)				Index
					As-is	1 month	2 months	3 months	
Matte tin/silver, 3.5% Ag	Brass	None	3	N	0	3	3	3	4.5
Matte tin/silver, 3.5% Ag	Olin 194	None	3	N	0	0	2	3	1.75
Matte tin/silver, 3.5% Ag	Alloy 42	None	3	N	0	2	4	4	4.5
Matte tin/silver, 3.5% Ag	Brass	Copper, 5 μm	3	N	4	4	4	4	10
Matte tin/silver, 3.5% Ag	Brass	Nickel, 2 μm	3	N	0	0	3	4	2.5
Matte tin/silver, 3.5% Ag	Olin 194	Copper, 5 μm	3	N	4	4	4	4	10
Matte tin/silver, 3.5% Ag	Olin 194	None	10	N	0	0	0	0	0
Matte tin/silver, 5% Ag	Brass	None	3	N	0	3	4	4	5.25
Matte tin/silver, 5% Ag	Olin 194	None	3	N	0	0	2	3	1.75
Matte tin/silver, 5% Ag	Alloy 42	None	3	N	0	4	4	4	6
Matte tin/silver, 5% Ag	Brass	Copper, 5 μm	3	N	3	3	3	3	7.5
Matte tin/silver, 5% Ag	Brass	Nickel, 2 μm	3	N	0	0	0	3	0.75
Matte tin/silver, 5% Ag	Olin 194	Copper, 5 μm	3	N	3	3	3	3	7.5
Matte tin/silver, 5% Ag	Olin 194	None	10	N	0	0	0	0	0
Matte tin/silver, 5% Ag									0
Matte pure tin (4)	Alloy 42	None	3	N	0	0	0	2	0.5
Matte pure tin (4)	Brass	None	3	N	1	4	4	4	7
Matte pure tin (4)	Olin 194	None	3	N	1	1	2	2	3.25
Matte pure tin (4)	Olin 194	None	10	N	0	0	0	0	0
Matte pure tin (4)	Olin 194	None	10	Y	0	0	0	2	0.5
Bright tin/copper (2), 2% Cu	Brass	Nickel, 2 μm	3	N	0	0	0	0	0
Bright tin/copper (2), 2% Cu	Olin 194	None	3	N	0	0	0	0	0
Bright tin/copper (2), 2% Cu	Olin 194	None	10	N	0	0	0	0	0
Matte tin/copper (3), 2% Cu	Olin 194	None	10	N	0	0	0	0	0
Matte tin/copper (3), 2% Cu	Olin 194	None	10	Y	0	0	0	0	0
Matte tin/copper (3), 2% Cu	Brass	None	3	N	0	4	4	4	6
Matte tin/copper (3), 2% Cu	Alloy 42	None	3	N	0	0	0	0	0
Matte tin/copper (3), 2% Cu	Olin 194	None	3	N	0	2	2	2	3